



# High-precision $Q_{EC}$ values of superallowed $0^+ \rightarrow 0^+$ $\beta$ -emitters $^{46}\text{Cr}$ , $^{50}\text{Fe}$ and $^{54}\text{Ni}$



P. Zhang<sup>a,b</sup>, X. Xu<sup>a</sup>, P. Shuai<sup>a</sup>, R.J. Chen<sup>a</sup>, X.L. Yan<sup>a</sup>, Y.H. Zhang<sup>a,\*</sup>, M. Wang<sup>a,\*</sup>, Yu.A. Litvinov<sup>c,a,\*</sup>, K. Blaum<sup>d</sup>, H.S. Xu<sup>a</sup>, T. Bao<sup>a</sup>, X.C. Chen<sup>a</sup>, H. Chen<sup>a,b</sup>, C.Y. Fu<sup>a,b</sup>, J.J. He<sup>e,a</sup>, S. Kubono<sup>a</sup>, Y.H. Lam<sup>a</sup>, D.W. Liu<sup>a,b</sup>, R.S. Mao<sup>a</sup>, X.W. Ma<sup>a</sup>, M.Z. Sun<sup>a,b</sup>, X.L. Tu<sup>a,d</sup>, Y.M. Xing<sup>a,b</sup>, J.C. Yang<sup>a</sup>, Y.J. Yuan<sup>a</sup>, Q. Zeng<sup>a,f</sup>, X. Zhou<sup>a,b</sup>, X.H. Zhou<sup>a</sup>, W.L. Zhan<sup>a</sup>, S. Litvinov<sup>c</sup>, G. Audi<sup>g</sup>, T. Uesaka<sup>h</sup>, Y. Yamaguchi<sup>h</sup>, T. Yamaguchi<sup>i</sup>, A. Ozawa<sup>j</sup>, B.H. Sun<sup>k</sup>, Y. Sun<sup>l</sup>, F.R. Xu<sup>m</sup>

<sup>a</sup> Key Laboratory of High Precision Nuclear Spectroscopy, Center for Nuclear Matter Science, Institute of Modern Physics, Chinese Academy of Sciences, Lanzhou 730000, People's Republic of China

<sup>b</sup> Graduate University of Chinese Academy of Sciences, Beijing, 100049, People's Republic of China

<sup>c</sup> GSI Helmholtzzentrum für Schwerionenforschung, Planckstraße 1, 64291 Darmstadt, Germany

<sup>d</sup> Max-Planck-Institut für Kernphysik, Saupfercheckweg 1, 69117 Heidelberg, Germany

<sup>e</sup> Key Laboratory of Optical Astronomy, National Astronomical Observatories, Chinese Academy of Sciences, Beijing, 100012, People's Republic of China

<sup>f</sup> University of Science and Technology of China, Hefei 230026, People's Republic of China

<sup>g</sup> CSNSM, Univ Paris-Sud, CNRS/IN2P3, Université Paris-Saclay, 91405 Orsay, France

<sup>h</sup> RIKEN Nishina Center, RIKEN, Saitama 351-0198, Japan

<sup>i</sup> Department of Physics, Saitama University, Saitama 338-8570, Japan

<sup>j</sup> Institute of Physics, University of Tsukuba, Ibaraki 305-8571, Japan

<sup>k</sup> School of Physics and Nuclear Energy Engineering, Beihang University, Beijing 100191, People's Republic of China

<sup>l</sup> Department of Physics and Astronomy, Shanghai Jiao Tong University, Shanghai 200240, People's Republic of China

<sup>m</sup> State Key Laboratory of Nuclear Physics and Technology, School of Physics, Peking University, Beijing 100871, People's Republic of China

## ARTICLE INFO

### Article history:

Received 17 October 2016

Received in revised form 4 January 2017

Accepted 20 January 2017

Available online 23 January 2017

Editor: V. Metag

### Keywords:

Storage rings

$Q_{EC}$  values

Superallowed  $0^+ \rightarrow 0^+$   $\beta$ -emitters

CVC test

## ABSTRACT

Short-lived  $^{46}\text{Cr}$ ,  $^{50}\text{Fe}$  and  $^{54}\text{Ni}$  were studied by isochronous mass spectrometry at the HIRFL-CSR facility in Lanzhou. The measured precision mass excesses ( $ME$ ) of  $^{46}\text{Cr}$ ,  $^{50}\text{Fe}$  and  $^{54}\text{Ni}$  are  $-29471(11)$  keV,  $-34477(6)$  keV and  $-39278(4)$  keV, respectively. The superallowed  $0^+ \rightarrow 0^+$   $\beta$ -decay  $Q$  values were derived to be  $Q_{EC}(^{46}\text{Cr}) = 7604(11)$  keV,  $Q_{EC}(^{50}\text{Fe}) = 8150(6)$  keV and  $Q_{EC}(^{54}\text{Ni}) = 8731(4)$  keV. The values for  $^{50}\text{Fe}$  and  $^{54}\text{Ni}$  are by one order of magnitude more precise than the adopted literature values. By combining the existing half-lives and branching ratios, we obtained the corrected  $\mathcal{F}t$  values to be  $\mathcal{F}t(^{50}\text{Fe}) = 3103(70)$  s and  $\mathcal{F}t(^{54}\text{Ni}) = 3076(50)$  s. The main contribution to the  $\mathcal{F}t$  uncertainties is now due to  $\beta$ -decay branching ratios, still, more high-precision measurements of the half-lives, the masses, and especially the branching ratios are needed in order to satisfy the requirements for a stringent CVC test.

© 2017 The Authors. Published by Elsevier B.V. This is an open access article under the CC BY license (<http://creativecommons.org/licenses/by/4.0/>). Funded by SCOAP<sup>3</sup>.

Nuclear  $\beta$  decays provide valuable information for studies in nuclear structure, nuclear astrophysics, as well as in the fundamental interactions and symmetries. One of the main parameters that characterizes  $\beta$  decay is the  $ft$  value with  $f$  being the

statistical rate function and  $t$  the partial half-life for a particular transition. For the superallowed  $0^+ \rightarrow 0^+$   $\beta$  decays occurring between nuclear analog states with nuclear spin-and-parity  $J^\pi = 0^+$  and isospin  $T = 1$ , precise determinations of  $ft$  values are since long an important research subject because these values sensitively probe the conserved vector current (CVC) hypothesis, set tight limits on the presence of scalar currents, and provide the most precise value for  $V_{ud}$ , the up-down quark-mixing element of the Cabibbo–Kobayashi–Maskawa (CKM) matrix (see, e.g., Refs. [1,2]).

\* Corresponding authors.

\*\* Corresponding author at: Institute of Modern Physics, Chinese Academy of Sciences, Nanchang Rd. 509, 730000 Lanzhou, P.R. China.

E-mail addresses: [yhzhang@impcas.ac.cn](mailto:yhzhang@impcas.ac.cn) (Y.H. Zhang), [wangm@impcas.ac.cn](mailto:wangm@impcas.ac.cn) (M. Wang), [y.litvinov@gsi.de](mailto:y.litvinov@gsi.de) (Yu.A. Litvinov).

The CVC hypothesis asserts that the weak vector coupling constant,  $G_V$ , is not renormalized in the nuclear medium. This indicates that the experimental  $ft$  value for a superallowed  $0^+ \rightarrow 0^+$   $\beta$  decay should be the same for all such transitions, independent of the nucleus. In reality, small corrections of radiative and isospin-symmetry-breaking have to be taken into account, and thus yielding a corrected  $\mathcal{F}t$  value defined as [3]:

$$\mathcal{F}t \equiv ft(1 + \delta'_R)(1 + \delta_{NS} - \delta_c) = \frac{K}{2G_V^2(1 + \Delta_R^V)}, \quad (1)$$

where  $K/(\hbar c)^6 = 8120.2787(11) \times 10^{-10} \text{ GeV}^{-4} \text{ s}$ ,  $\Delta_R^V$  is the transition-independent part of the radiative correction,  $\delta'_R$  and  $\delta_{NS}$  are the transition-dependent parts of the radiative correction, and  $\delta_c$  is the isospin-symmetry-breaking correction. From this equation, one sees that each measured transition establishes an individual value for  $G_V$  and, if the CVC hypothesis holds, all the  $\mathcal{F}t$  values should be identical within uncertainties regardless of the specific nuclei involved. In confirmation of the CVC hypothesis, the value for  $G_V$  determined from the  $\mathcal{F}t$  values can be used in combination with  $G_F$ , the weak-interaction constant determined from purely leptonic muon decays [2], to calculate the  $V_{ud}$  matrix element, which is needed for testing the unitarity of the CKM matrix, a fundamental property of the electroweak Standard Model [1,2].

For the determination of an  $ft$  value one requires the total transition energy,  $Q_{EC}$ , the half-life,  $T_{1/2}$ , of the parent state, and the branching ratio,  $BR$ , for the particular transition of interest. The  $Q_{EC}$  value is required to determine the statistical rate function,  $f$ , while the half-life and branching ratio are combined to yield the partial half-life,  $t$ . Note that  $f$  depends on the fifth power of the  $Q_{EC}$  value [4]. Thus it is essential to determine the  $Q_{EC}$  with the highest precision possible.

Twenty superallowed  $0^+ \rightarrow 0^+$   $\beta$  decays have been critically surveyed recently [2] and their  $\mathcal{F}t$  values evaluated. The authors recommended an average  $\mathcal{F}t$  value based on the 14 most precise values. Soon after this survey, a new measurement of  $\beta$  decays of  $^{42}\text{Ti}$ ,  $^{46}\text{Cr}$ ,  $^{50}\text{Fe}$ , and  $^{54}\text{Ni}$  has been reported [5]. A similar survey was performed for these four nuclei in Ref. [6]. The authors called for precision measurements of the three quantities for each of the four  $T_z = -1$   $fp$ -shell nuclei in order to be able to use more  $0^+ \rightarrow 0^+$   $\beta$ -decay data for the test of the CVC hypothesis and for the comparison of the  $ft$  values of mirror transitions. The mass of  $^{42}\text{Ti}$  has been measured with 0.28 keV uncertainty at the JYFLTRAP Penning-trap facility [7], while those for  $^{46}\text{Cr}$ ,  $^{50}\text{Fe}$ , and  $^{54}\text{Ni}$  were only measured about 40 years ago either from a reaction excitation function [8] or from the  $Q$  values of  $(^4\text{He}, ^8\text{He})$  reactions [9]. The uncertainties of these measurements are far beyond the required precision of about 0.1% [2,6]. The mass of  $^{54}\text{Ni}$  was addressed at the JYFLTRAP, but no result could be obtained due to a very low production yield [10].

In this Letter we report high-precision mass measurements of short-lived  $T_z = -1$   $fp$ -shell nuclei performed by employing the storage-ring based isochronous mass spectrometry method. By tuning the experimental cooler storage ring (CSRe) into the isochronous ion-optical setting centered on  $^{52}\text{Co}$ , a relative mass precision of  $\sim 1 \times 10^{-7}$  has been achieved for  $^{50}\text{Fe}$  and  $^{54}\text{Ni}$ . These are the heaviest  $T_z = -1$  nuclei for which the masses are known with such a high precision. We report here the new masses for  $^{50}\text{Fe}$  and  $^{54}\text{Ni}$  which are 10 times more precise than the previously accepted values [11]. By combining our new results with the known masses of the associated  $T = 1$  isobaric analog states (IAS) in the  $T_z = 0$  daughter nuclei [11], the  $Q_{EC}$ -values of the superallowed  $\beta$ -decay of  $^{50}\text{Fe}$  and  $^{54}\text{Ni}$  are newly determined.

The experiment was conducted at the HIRFL-CSR facility, which is an acceleration complex consisting of a separated sector cyclotron (SSC,  $K = 450$ ), a sector-focusing cyclotron (SFC,  $K = 69$ ),

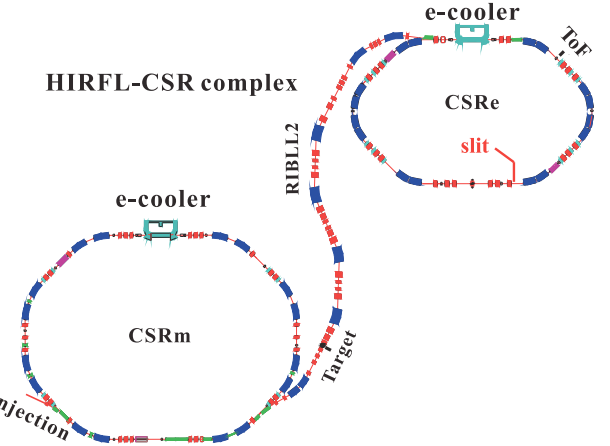


**Fig. 1.** (Color online.) The high-energy part of the HIRFL-CSR complex at IMP indicating the synchrotron CSRm, the in-flight fragment separator RIBLL2, and the experimental storage ring CSRe.

a main cooler-storage ring (CSRm) operating as a heavy-ion synchrotron, and an experimental ring CSRe [12]. The high-energy part of the facility is schematically shown in Fig. 1. The CSRm has a circumference of 161 m and a maximal magnetic rigidity  $B\rho$  of 10 Tm. The CSRe has a circumference of 128.8 m and a maximal magnetic rigidity of 8.4 Tm [12]. The  $B\rho$  acceptance of CSRe in the isochronous mode is  $\pm 0.2\%$ .

In this experiment, a 467.91 MeV/u  $^{58}\text{Ni}^{19+}$  primary beam was focused onto a  $\sim 15$  mm thick beryllium target placed in front of the in-flight fragment separator RIBLL2. The reaction products from projectile fragmentation of  $^{58}\text{Ni}$  were analyzed [13] by RIBLL2 and a cocktail beam including the ions of interest was injected into the CSRe. According to LISE++ simulations [14], the ions of interest have the velocity distribution centered at  $\gamma = 1.400$ . Therefore, the CSRe was tuned into the isochronous ion-optical mode [15–17] with the transition energy of  $\gamma_t = \gamma = 1.400$ . At these kinetic energies, the fragments are predominantly fully-ionized according to the estimations with a specialized CHARGE code [18].

Both RIBLL2 and CSRe were set to a fixed magnetic rigidity of  $B\rho = 5.8574$  Tm to allow for an optimal transmission of the  $T_z = -1$  nuclides centered on  $^{52}\text{Co}$ . The  $\gamma_t$  deviates from 1.400 at the edges of the CSRe aperture. Similar behavior can be seen in Ref. [15] on the example of the storage ring at GSI, Darmstadt. Therefore, we restricted the range of orbits by inserting a slit at the position with high dispersion (see Fig. 1). The latter was estimated to be about 20 m. The slit opening was 60 mm corresponding to the momentum acceptance of the CSRe of  $\Delta p/p \pm 0.15\%$ . As a result, the resolving power of the acquired spectra was considerably improved leading to clear separation of the ground-state  $^{52}\text{Co}$  from its low-lying isomer [19]. We note that in addition to the ions of interest, other nuclides within the acceptance of the RIBLL2-CSRe system were transmitted and stored as well. Typically, about ten ions were stored simultaneously in each injection. The nuclides with well-known masses have been used as reference ions.

The revolution times of the ions stored in CSRe were measured using a timing detector [20] installed inside the CSRe aperture. For a single passage of an ion, the time resolution of the detector is about 50 ps, and the detection efficiency varies from  $\sim 20\%$  to  $\sim 70\%$  depending on the charge state and overall number of stored ions (see Refs. [17,20] for details). For each injection the measurement time was set to 300  $\mu\text{s}$ , which corresponds to  $\sim 500$  revolutions of the ions. The ions that circulated for more than 100  $\mu\text{s}$  were considered in the analysis. This is different from previous analyses [17,21–23], where the minimum time of 186  $\mu\text{s}$  was

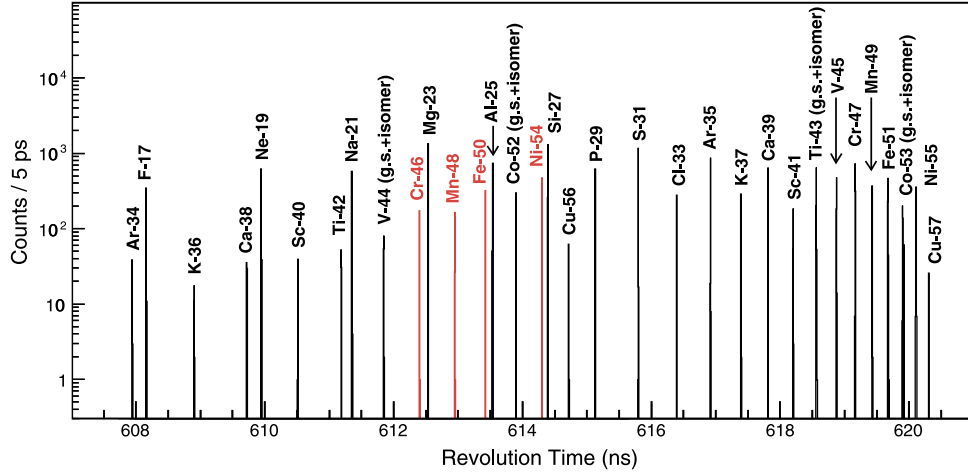


**Fig. 2.** (Color online.) Part of the revolution time spectrum zoomed in at a time window of  $607 \text{ ns} \leq t \leq 621 \text{ ns}$ . The red peaks indicate those nuclei for which masses are reported in this work.

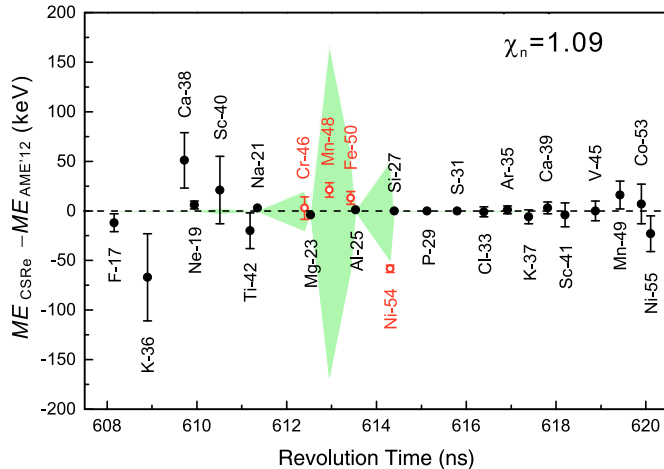


**Fig. 3.** (Color online.) Differences between experimental  $ME$  values determined in this work and those from the atomic-mass evaluation AME'12. The green shadows indicate the  $1\sigma$  error in AME'12.

applied. Thus, the number of ions used in the analysis could be increased.

The resolving power of the CSRe mass spectrometry was deteriorated by magnetic field instabilities which caused small shifts of the entire revolution time spectra measured in different injections. A correction method [24] was applied in the data analysis to correct for the influence of unstable magnetic fields. Fig. 2 illustrates a part of the corrected spectrum in a time window of  $607 \text{ ns} \leq t \leq 621 \text{ ns}$ . The identification of the peaks in the spectrum is described in Ref. [17].

We used 21 nuclides observed in the time range of  $607 \text{ ns} \leq t \leq 621 \text{ ns}$  with known mass uncertainties of less than 5 keV [25] to fit their  $m/q$  values versus the revolution time by employing a third order polynomial, giving a mass calibration to the revolution time spectrum. The unknown mass values were determined by interpolating the fit function to the corresponding revolution times. In order to estimate possible systematic errors, we re-determined the masses for each of the 21 nuclides by calibrating the spectrum with the other 20 nuclides. The differences between our mass excess ( $ME$ ) values and the literature ones [25] are compared in Fig. 3. We calculated the normalized  $\chi_n$  defined as:

**Table 1**

Experimental  $ME$  values obtained in this work and values from the atomic-mass evaluation AME'12 [25]. The deviations  $\delta ME = ME_{\text{CSRe}} - ME_{\text{AME'12}}$  are given in the last column. Also listed are the numbers of identified ions  $N$ , standard deviation,  $\sigma_t$ , and FWHM values of the revolution time peaks (see Fig. 2). The latter are converted in keV through mass calibration.

Atom	$N$	$\sigma_t$ (ps)	FWHM (keV)	$ME_{\text{CSRe}}$ (keV)	$ME_{\text{AME'12}}$ (keV)	$\delta ME$ (keV)
$^{42}\text{Ti}$	85	1.33	403	-25125(19)	-25104.66(28)	-20
$^{46}\text{Cr}$	195	1.13	373	-29471(11)	-29474(20)	+3
$^{48}\text{Mn}$	198	0.69	242	-29299(7)	-29320(170)	+21
$^{50}\text{Fe}$	343	0.76	277	-34477(6)	-34490(60)	+13
$^{54}\text{Ni}$	688	0.54	226	-39278(4)	-39220(50)	-58

$$\chi_n = \sqrt{\frac{1}{n_f} \sum_{i=1}^{21} \frac{[(ME)_{\text{CSRe},i} - (ME)_{\text{AME},i}]^2}{\sigma_{\text{CSRe},i}^2 + \sigma_{\text{AME},i}^2}}, \quad (2)$$

with  $n_f = 21$  being the number of degrees of freedom. The calculated value of  $\chi_n = 1.09$  is within the expected range of  $\chi_n = 1 \pm 0.15$  at  $1\sigma$  confidence level, indicating that no additional systematic errors have to be considered. The  $ME$  values obtained in this work are presented in Table 1 together with the values from AME'12 [25] for comparison. The differences are given in the last column of Table 1 and shown in Fig. 3. The larger uncertainties, e.g., for  $^{36}\text{K}$ ,  $^{38}\text{Ca}$ ,  $^{40}\text{Sc}$  and  $^{42}\text{Ti}$ , are due to low statistics.

Three points should be emphasized here: Firstly, our measurement yields  $ME^{(48)\text{Mn}} = -29299(7)$  keV, which is 24 times more precise than the adopted value in AME'12 [25] (see Table 1). This precise result can independently be verified by using the recent data from the  $\beta$  decay studies of  $^{48}\text{Fe}$  [26]. In that experiment, both  $\beta$ -delayed protons and  $\beta$ -delayed  $\gamma$ 's of  $^{48}\text{Fe}$  decay have been measured and assigned as being due to the de-excitation of the  $T = 2$  isobaric analog state in the  $T_z = -1$  nucleus  $^{48}\text{Mn}$ . Therefore the ground-state  $ME$  value of  $^{48}\text{Mn}$  can be obtained through,

$$\begin{aligned} ME^{(48)\text{Mn}} &= ME^{(47)\text{Cr}} + ME^{(1)\text{H}} + E_p^{\text{c.m.}} - E_\gamma^{\text{sum}} \\ &= [-34561(7) + 7289 + 1018(10) - 3036.5(1.5)] \text{ keV} \\ &= -29291(12) \text{ keV}, \end{aligned} \quad (3)$$

with  $E_p^{\text{c.m.}}$  being the proton decay energy in the center-of-mass system, and  $E_\gamma^{\text{sum}}$  the summed energy of three sequential  $\gamma$  transitions from the IAS in  $^{48}\text{Mn}$ . The deduced  $ME$  value for  $^{48}\text{Mn}$  agrees well with our direct measurement. Secondly, as shown in Fig. 2, the revolution times of  $^{46}\text{Cr}$ ,  $^{50}\text{Fe}$ , and  $^{54}\text{Ni}$  are very close to

**Table 2**

A comparison of the determined superallowed  $Q_{EC}$  values, statistical rate function  $f$ , and the corrected  $\mathcal{F}t$  values with the latest survey of superallowed nuclear  $\beta$  decay [6].

Fermi transition	$Q_{EC}$ (keV)	$f$	$\mathcal{F}t$ (s)	Ref.
$^{46}\text{Cr} \rightarrow ^{46}\text{V}$	7604(11)	10683(84)	3141(100)	this work
$^{46}\text{Cr} \rightarrow ^{46}\text{V}$	7600(20)	10660(150)	3130(110)	[6]
$^{50}\text{Fe} \rightarrow ^{50}\text{Mn}$	8150(6)	15060(60)	3103(70)	this work
$^{50}\text{Fe} \rightarrow ^{50}\text{Mn}$	8139(60)	14950(600)	3080(140)	[6]
$^{54}\text{Ni} \rightarrow ^{54}\text{Co}$	8731(4)	21130(50)	3076(50)	this work
$^{54}\text{Ni} \rightarrow ^{54}\text{Co}$	8787(50)	21850(670)	3180(110)	[6]

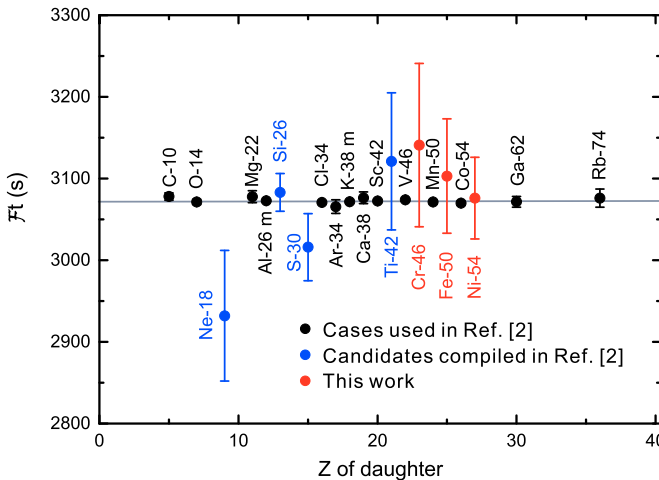


**Fig. 4.** (Color online.)  $\mathcal{F}t$  values plotted as a function of the charge of the daughter nucleus,  $Z$ . The black circles stand for the fourteen cases used in Ref. [2], the blue circles for the potential candidates compiled in Ref. [2], and the red ones from this work.

those of  $^{23}\text{Mg}$ ,  $^{25}\text{Al}$ , and  $^{27}\text{Si}$ , respectively. The re-determined mass excesses of the latter are in excellent agreement with their precise literature values. Thirdly, our measured mass for  $^{54}\text{Ni}$  differs by 58 keV, i.e.,  $1.2\sigma$ , from the adopted value [11]. Still its corrected  $\mathcal{F}t$  value has been deduced to be very close to the recommended one when using our results to calculate the statistical rate function  $f$ .

Using the  $ME$  values of  $^{46}\text{Cr}$ ,  $^{50}\text{Fe}$ , and  $^{54}\text{Ni}$  obtained in this work and the adopted  $ME$  values of the corresponding  $T = 1$  IAS's in their  $\beta$ -decay daughters  $^{46}\text{V}$ ,  $^{50}\text{Mn}$ , and  $^{54}\text{Co}$  [11], we calculated the  $Q_{EC}$  values, see Table 2. The parameterization formulas of Eqs. (12) through (14) given in Ref. [6] were used to calculate each statistical rate function  $f$ . The partial half-lives and associated theoretical correction terms,  $\delta'_R$  and  $\delta_c - \delta_{NS}$ , have been collected in Ref. [6], which allowed us to calculate the corrected  $\mathcal{F}t$  values using Eq. (1). The results are given in Table 2 and depicted in Fig. 4.

It can be seen that our new results are in a good agreement with Ref. [6], but with much improved precision. The uncertainties in the statistical rate functions for  $^{50}\text{Fe}$  and  $^{54}\text{Ni}$  are reduced by one order of magnitude reaching a level of  $\sim 0.3\%$ . Consequently, the uncertainties of the  $\mathcal{F}t$  values are also reduced as shown in Table 2. We note that the new  $\mathcal{F}t = 3076(50)$  s for  $^{54}\text{Ni}$  is by 3.2% smaller than the previous one [6] now agreeing well with the latest averaged value of  $\mathcal{F}t = 3072.27(72)$  s [2].

The present uncertainties of the  $\mathcal{F}t$ -values are still too large to be used for a critical test of the CVC hypothesis. Fig. 5 presents fractional uncertainties of the experimental and theoretical input factors contributing to the final  $\mathcal{F}t$  values for the three discussed superallowed transitions. It is seen that the limiting factor is now

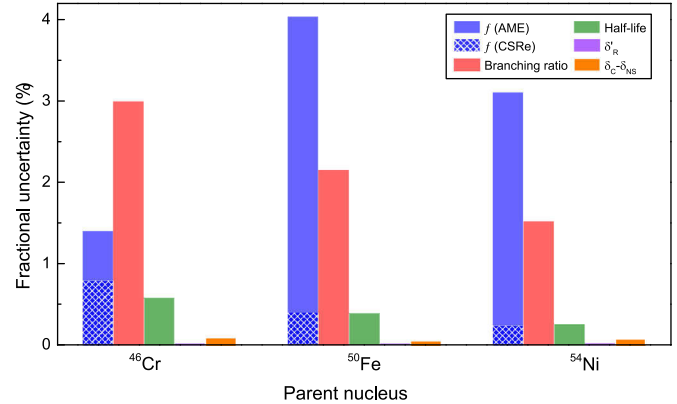


**Fig. 5.** (Color online.) Fractional uncertainties of the experimental and theoretical input factors contributing to the final  $\mathcal{F}t$  values of the superallowed transitions of  $^{46}\text{Cr}$ ,  $^{50}\text{Fe}$  and  $^{54}\text{Ni}$ . The data are from this work and from Refs. [2,6].

the uncertainty of the  $BR$ . Therefore high-precision measurements of superallowed  $\beta$ -decay branching ratios are essential, at least for the above-mentioned cases, in order to improve the precision in their  $\mathcal{F}t$ .

In conclusion, the  $T_z = -1$  nuclei,  $^{46}\text{Cr}$ ,  $^{50}\text{Fe}$ , and  $^{54}\text{Ni}$  were produced by the projectile fragmentation of  $^{58}\text{Ni}$  beam, and their atomic masses were measured using the storage-ring based isochronous mass spectrometry technique. Our results are in excellent agreement with the latest atomic-mass evaluation AME/12 [25], but with much improved precision. The new masses of  $^{50}\text{Fe}$  and  $^{54}\text{Ni}$  are one order of magnitude more precise than the adopted values [25]. We have obtained the superallowed Fermi decay  $Q_{EC}$  values and calculated the statistical rate functions. Taking into account the radiative and isospin-symmetry-breaking corrections, we have calculated the corrected  $\mathcal{F}t$  values in order to provide new data for testing the conserved vector current hypothesis. The obtained  $\mathcal{F}t$  values are much more precise and are in excellent agreement with the averaged value of  $\mathcal{F}t = 3072.27(72)$  s [2]. Owing to the accurate  $Q$ -value determination in this work, the uncertainties in  $\mathcal{F}t$  values for  $^{50}\text{Fe}$  and  $^{54}\text{Ni}$  are now dominated by the corresponding  $\beta$ -decay branching ratios. The present work is a step-forward for the heaviest  $T_z = -1$  pf nuclei, and more high-precision measurements of the half-lives, the masses, and especially the branching ratios are needed in order to satisfy the requirements for a stringent CVC test.

### Acknowledgements

The authors thank the staffs in the accelerator division of IMP for providing stable beam. This work is supported in part by the Major State Basic Research Development Program of China (Contract No. 2013CB834401), the National Key Program for S&T Research and Development (2016YFA0400504), the NSFC grants U1232208, U1432125, 11205205, 11035007, 11235001, 11320101004, 11575007, 11575112, 11135005, the Chinese Academy of Sciences, and the Helmholtz–CAS Joint Research Group (HCJRG-108). Y.A.L. acknowledges the support by the CAS President's International Fellowship Initiative Grant (2016VMA043). K.B. acknowledges support by the Nuclear Astrophysics Virtual Institute (NAVI) of the Helmholtz Association. X.X. thanks the support from CAS "Light of West China" Program.

### References

- [1] J.C. Hardy, I.S. Towner, Phys. Rev. Lett. 94 (2005) 092502.
- [2] J.C. Hardy, I.S. Towner, Phys. Rev. C 91 (2015) 025501.
- [3] I.S. Towner, J.C. Hardy, Phys. Rev. C 82 (2010) 065501.

- [4] I.S. Towner, J.C. Hardy, Phys. Rev. C 91 (2015) 015501.
- [5] F. Molina, et al., Phys. Rev. C 91 (2015) 014301.
- [6] I.S. Towner, J.C. Hardy, Phys. Rev. C 92 (2015) 055505.
- [7] T. Kurtukian Nieto, et al., Phys. Rev. C 91 (2009) 035502.
- [8] J. Zioni, et al., Nucl. Phys. A 181 (1972) 465.
- [9] R.E. Tribble, et al., Phys. Rev. C 16 (1977) 917.
- [10] A. Kankainen, et al., Phys. Rev. C 82 (2010) 034311.
- [11] G. Audi, et al., Chin. Phys. C 36 (2012) 1157.
- [12] J.W. Xia, et al., Nucl. Instrum. Methods Phys. Res., Sect. A 488 (2002) 11.
- [13] H. Geissel, et al., Nucl. Instrum. Methods Phys. Res., Sect. B 70 (1992) 286.
- [14] O.B. Tarasov, D. Bazin, Nucl. Instrum. Methods Phys. Res., Sect. B 266 (2008) 4657.
- [15] M. Hausmann, et al., Nucl. Instrum. Methods Phys. Res., Sect. A 446 (2000) 569.
- [16] X.L. Tu, et al., Phys. Rev. Lett. 106 (2011) 112501.
- [17] X.L. Tu, et al., Nucl. Instrum. Methods Phys. Res., Sect. A 654 (2011) 213.
- [18] C. Scheidenberger, et al., Nucl. Instrum. Methods Phys. Res., Sect. B 142 (1998) 441.
- [19] X. Xu, et al., Phys. Rev. Lett. 117 (2016) 182503.
- [20] B. Mei, et al., Nucl. Instrum. Methods Phys. Res., Sect. A 624 (2010) 109.
- [21] Y.H. Zhang, et al., Phys. Rev. Lett. 107 (2012) 102501.
- [22] X.L. Yan, et al., Astrophys. J. Lett. 766 (2013) L8.
- [23] P. Shuai, et al., Phys. Lett. B 735 (2014) 327.
- [24] P. Shuai, et al., arXiv:1407.3459.
- [25] M. Wang, et al., Chin. Phys. C 36 (2012) 1603.
- [26] S.E.A. Orrigo, et al., Phys. Rev. C 93 (2016) 044336.